Numerical quantification of damage accumulation resulting from blanking in multi-phase steel

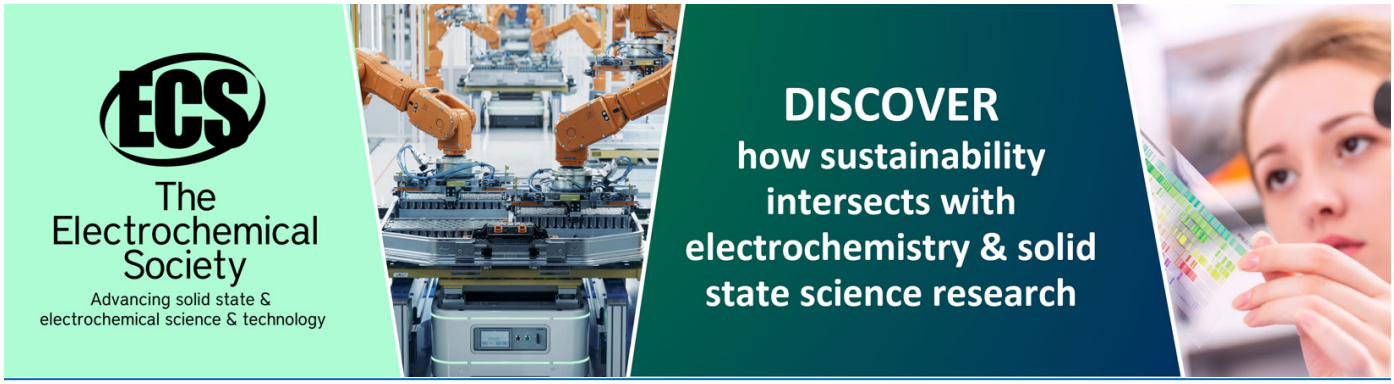

IOP Conf. Series: Materials Science and Engineering **418** (2018) 012058 doi:10.1088/1757-899X/418/1/012058

Numerical quantification of damage accumulation resulting from blanking in multi-phase steel

N Habibi[1], F Pütz[1], M Könemann[1], V Brinnel[1], S Münstermann[1], M Feistle[2] and W Volk[2]

[1] Steel Institute (IEHK), RWTH Aachen University, Germany

[2] Chair of Metal Forming and Casting, Technical University of Munich, Germany

Niloufar.habibi@iehk.rwth-aachen.de

Abstract. The high potentials of utilizing high strength steels in the automotive industry have been proved. However, there are still some unsolved challenges. Forming of a component that has been produced by blanking is one of these. Blanking is commonly used in sheet metal forming as the initial cutting process. Yet, it introduces damage into the blanked edges that in subsequent forming steps may lead to crack formation. This problem arises in particular in modern multi-phase steels and can currently not be avoided thoroughly due to a lack of understanding of the relevant influences. In the present work, the effects of the blanking process on an HCT980XD sheet were therefore numerically investigated. To achieve this, the *Edge-Fracture-Tensile-Test* method was simulated. By using this method, a conventional uniaxial tensile specimen is manufactured with one milled side and one blanked side. This allows to highlight the effect of blanking in a subsequent tensile test. In order to investigate the damage process, the coupled Modified-Bai-Wierzbicki model was applied to simulate first the blanking process and then the tensile test. The results revealed that during the blanking process, the failure initiated from the surface elements near the punch and propagated through the thickness. Meanwhile, another crack initiated from the opposite side of the sheet. The elements of these cracks experienced near pure-shear condition at both damage initiation and fracture moments. At the end of this step, the remaining damage, which is considered as the predamage of the next step, was higher in the middle of thickness. During the subsequent uniaxial tension, the crack in the specimen initiated at a shear cut edge and crossed the width. The possible detailed resolution of loading paths and crack formation shows that the damage mechanics simulation provides researchers with a powerful tool for assessing limit states in forming processes.

1. Introduction

High Strength Steel (HSS) sheets are widely used in automotive industries. They mostly undergo several complicated forming processes to obtain their final shape. Blanking is a common forming process which is used for the initial cutting. This process imposes some adverse effects on the shear cut edge, which become profound during the subsequent forming processes. Some materials like multi-phase steels are more sensitive to edge properties and blanking may result in formation of premature cracks in their edge [1]. These induce component failure during the forming process ahead of the expected forming limits, which are determined by the conventional methods.

Prediction of forming limits especially by using computer-aided engineering method is highly beneficial for increasing productivity by reducing cost and effort of production design and improving its accuracy. There are few experimental testing techniques, which have been so far proposed to measure edge crack sensitivity. The most common one is the Hole Expansion Test (HET) which has been widely used for HSS sheets [2-4]. However, only a few numerical studies have been conducted on the edge crack sensitivity through HET [5], especially by considering the cutting impacts [6-9]. Sartkulvanich et al. [7] illustrated how metal flow, strains and stresses in cutting affect edge cracking through the following stretch flanging by using 2D finite element method and a simple uncoupled damage model. However the simulation and experimental results showed good agreement with each other, applying 3D model along with a simple uncoupled damage model (critical plastic strain at fracture) can describe the localized edge cracking more precisely. Hu et al [8] predicted the effect of cut conditions on hole expansion ratio of an aluminum alloy using 3D finite element method. The results showed that by increasing the clearance, accuracy of the predictions decreased. They also predicted tensile stretchability for the same material by implementing Rice-Tracey uncoupled damage model [9]. They showed that the prediction was not accurate for clearance more than 10%.

Recently a promising experimental method has been developed by the Chair of Metal Forming and Casting of the Technical University of Munich, called *Edge-Fracture-Tensile-Test* (EFTT). In this method, influences of the blanking process on the formability of the shear cut edge are investigated by manufacturing a conventional uniaxial tensile specimen which contains a milled side and an edge cut side. Figure 1 illustrates the manufacturing steps of an EFTT specimen. This testing technique represents several advantages, for instance providing a frictionless medium, avoiding any strain gradients ahead of local necking, offering a convenient study on the shear cut edge, and showing a high reproducibility [10, 11]. These characteristics make this method a favorable model for numerical investigations, however no attempts have been made in this regard yet. Hence, the objective of the present work is to study EFTT process numerically and assess the accuracy of results by comparing with the experiments.

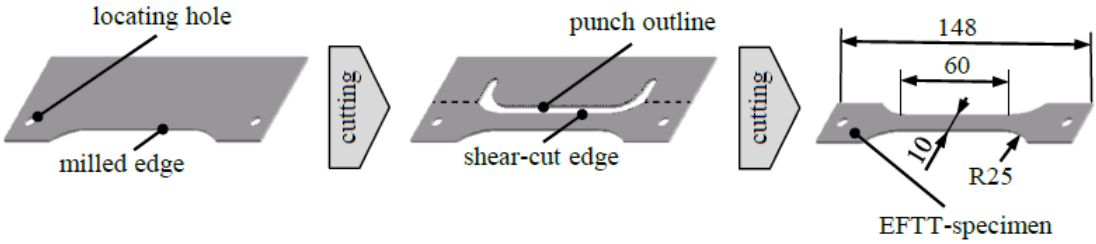

Figure 1. Manufacturing process of a blanked EFTT specimen with a closed cutting lines [12].

2. Methods

2.1. Plasticity model

In order to describe the material's behavior in the simulations, a plasticity-damage model was employed based on a combined experimental and numerical approach. In this regard, the Modified-Bai-Wierzbicki (MBW) damage mechanics model, presented by Wu et al. [13], was applied and the damage parameters for different stress states were determined. In this plasticity model, equation (1), damage appears as strain-softening in the material behavior.

$$\Phi = \sigma_e - (1-D)\sigma_{yld} \leq 0 \tag{1}$$

Herein, Φ is the flow potential, σ_e is the equivalent stress, σ_{yld} is the yield stress, and D is the ductile damage variable. According to the damage model, equation (2), the initial material is assumed to be defect-free and only strain-hardening contributes to the deformation. The damage initiates when the equivalent plastic strain, $\bar{\varepsilon}^{p}$, reaches a threshold value, $\bar{\varepsilon}^{i}$ as defined in equation (3). Afterwards,

the damage propagates linearly in proportion to the flow stress at damage initiation, $\sigma_{y,i}$, and an energy-dissipation coefficient, G_f. The damage evolves until the fracture occurs at equivalent plastic strain of $\bar{\varepsilon}^f$, which is fulfilled by equation (4). It is worth mentioning that the damage model is defined in terms of stress-triaxiality, η, and normalized Lode angle parameter, $\bar{\theta}$, to describe stress-state of the material during the deformation. Note that all C_i and D_i parameters are materials' constants.

$$D = \begin{cases} 0, & \bar{\varepsilon}^p \le \bar{\varepsilon}^i \\ \dfrac{\sigma_{y,i}}{G_f} \displaystyle\int_{\bar{\varepsilon}^i}^{\bar{\varepsilon}^p} d\bar{\varepsilon}^p & \bar{\varepsilon}^i < \bar{\varepsilon}^p \le \bar{\varepsilon}^f \end{cases} \tag{2}$$

$$\bar{\varepsilon}^i = \left(C_1 e^{-C_2\eta} - C_3 e^{-C_4\eta}\right)\bar{\theta}^2 + C_3 e^{-C_4\eta} \tag{3}$$

$$\int_{\bar{\varepsilon}^i}^{\bar{\varepsilon}^f} \frac{dD}{\left(D_1 e^{-D_2\eta} - D_3 e^{-D_4\eta}\right)\bar{\theta}^2 + D_3 e^{-D_4\eta}} = 1 \tag{4}$$

2.2. Material and parameter identification

Dual-phase HCT980XD steel sheets, DP1000 according to DIN EN 10346, were received with the thickness of 1.5 mm. Its mechanical properties were evaluated through different uniaxial loading conditions along with ARAMIS digital image correlation (DIC) analysis. The hardening parameters were calculated directly by fitting Hollomon model (equation (5)) on the homogenous plastic part of the flow curve, which was extracted from the results of uniaxial tensile tests. The damage parameters were calibrated using an inverse strategy, i.e. parameters were determined by minimizing the difference between experimental and simulation results, here particularly the results of force-displacement were considered. Since MBW parameters are non-unique, a wide range of stress states should be examined to calculate the parameters properly. Therefore, notched dog bone, plane-strain, central hole, and shear specimens were tested along with the parallel numerical simulations using finite-element software Abaqus/Explicit 2017, figure 2 and 3. In all the simulations, eight-node reduced-integration solid elements of type C3D8R were employed. In order to minimize the computational time, a mesh size of 0.1 mm was applied only on those regions of samples which are exposed higher plastic straining. The material parameters are summarized in table 1.

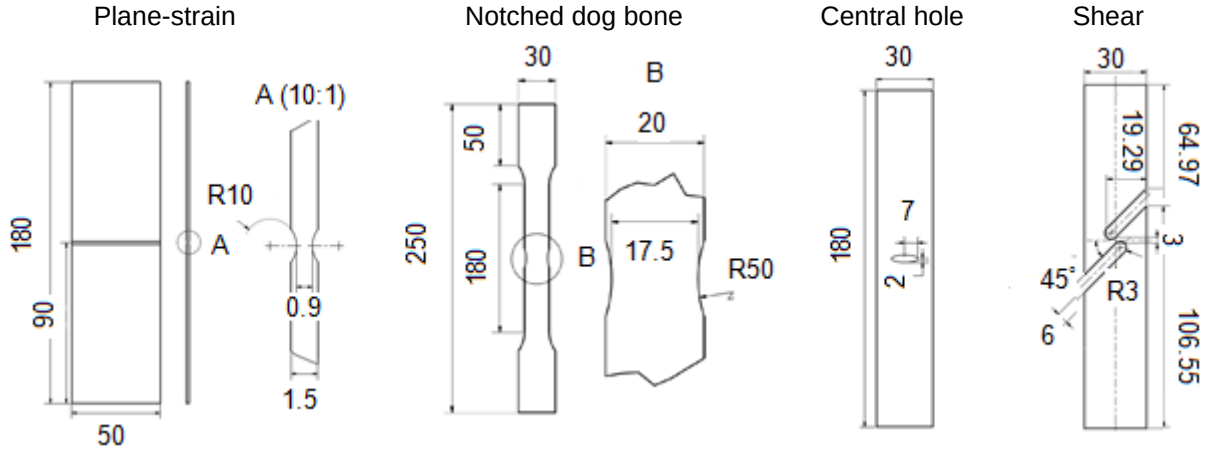

Figure 2. The geometries of different specimens (all dimensions are in mm).

Table 1. Mechanical properties of the investigated material.

Parameter	E (GPa)	ν	$R_{P0.2}$ (MPa)	k (MPa)	n_H
Value	210	0.3	693	1476	0.10
Regime	Elastic		Plastic		
Identification	Direct				

Parameter	C_1	C_2	C_3	C_4	G_f	D_1	D_2	D_3	D_4
Value	0.4	1	0.1	1.5	6500	0.15	1.5	0.08	1.5
Regime	Damage initiation				Damage propagation	Fracture			
Identification	Inverse								

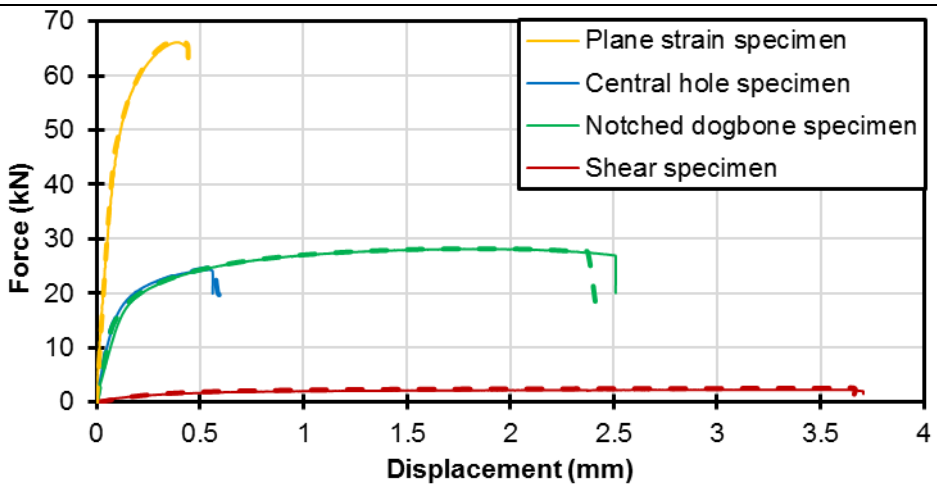

Figure 3. The force-displacement curves of experiments (solid lines) and simulations (dashed lines).

$$\sigma_e = k \cdot \left(\bar{\varepsilon}^p\right)^{n_H} \tag{5}$$

2.3. Simulation of Edge-Fracture-Tensile-Test

The numerical simulations of a two-stage *Edge-Fracture-Tensile-Test* were performed for a set-up with sharp cutting edges tool (edge radii of 0.05 mm) and a die clearance of 15%. In order to reduce the computation time, only half of the symmetric model was modeled, figure 4. In the blanking process, the die, punch, and blank holder were considered as discrete rigid parts, and the sheet was modeled as a deformable homogenous solid. Friction between the tools and the sheet was considered as the Coulomb model with a coefficient of 0.1 [9]. The contact pairs were defined as a surface-to-surface algorithm. However, the contacts between new surfaces which are created during blanking process and the tool were defined as a node-to-surface algorithm. Since the applied damage model is a local model and influenced by the mesh size, mesh size of 0.1 mm was used in the critical regions of the sheet like the models which were used for the parameter calibration. In order to apply homogenous force on the sheet during the blanking process, finer elements were defined in the contact regions of the tool. An optimal clamping force was chosen such that the blank was neither drew in nor torn improperly during the blanking process. For the second stage, the tensile test on the produced sample, the unnecessary parts of the sheet were deleted and uniaxial tension was quasi-statically employed on the gauge length to assess the effect of the blanked edge on the formability of the material.

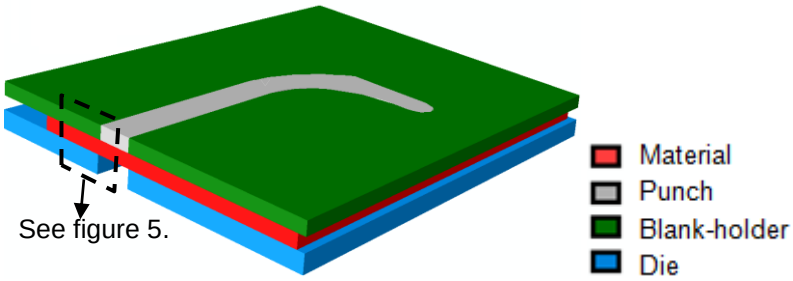

Figure 4. The assembly model of half *Edge-Fracture-Tensile-Test* for the blanking stage.

2.4. EFTT process: Blanking stage

Blanking is the first stage of EFTT process. Through this stage, the blanked edge of the tensile specimen is manufactured. The gradual formation of the blanked edge is shown in figure 5, in terms of stress-triaxiality and Normalized Lode-angle parameter, i.e. the stress-state. Moreover, the geometrical features of the edge, which are created during the blanking process, are shown in figure 6. By penetration of the punch through the material, an elastic deformation began and turned into a plastic deformation. When the equivalent plastic strain reached the critical value, damage occurred. Up to this moment, the imposed elements experienced shear stress-state, since both η and $\bar{\theta}$ are about 0, figure 5(a). The stress-state remained in near shear mode while the damage propagated though the material and accumulated, figure 5(b). Up to a crack initiated, the upper area was exposed bending effects. This area is called rollover [14].

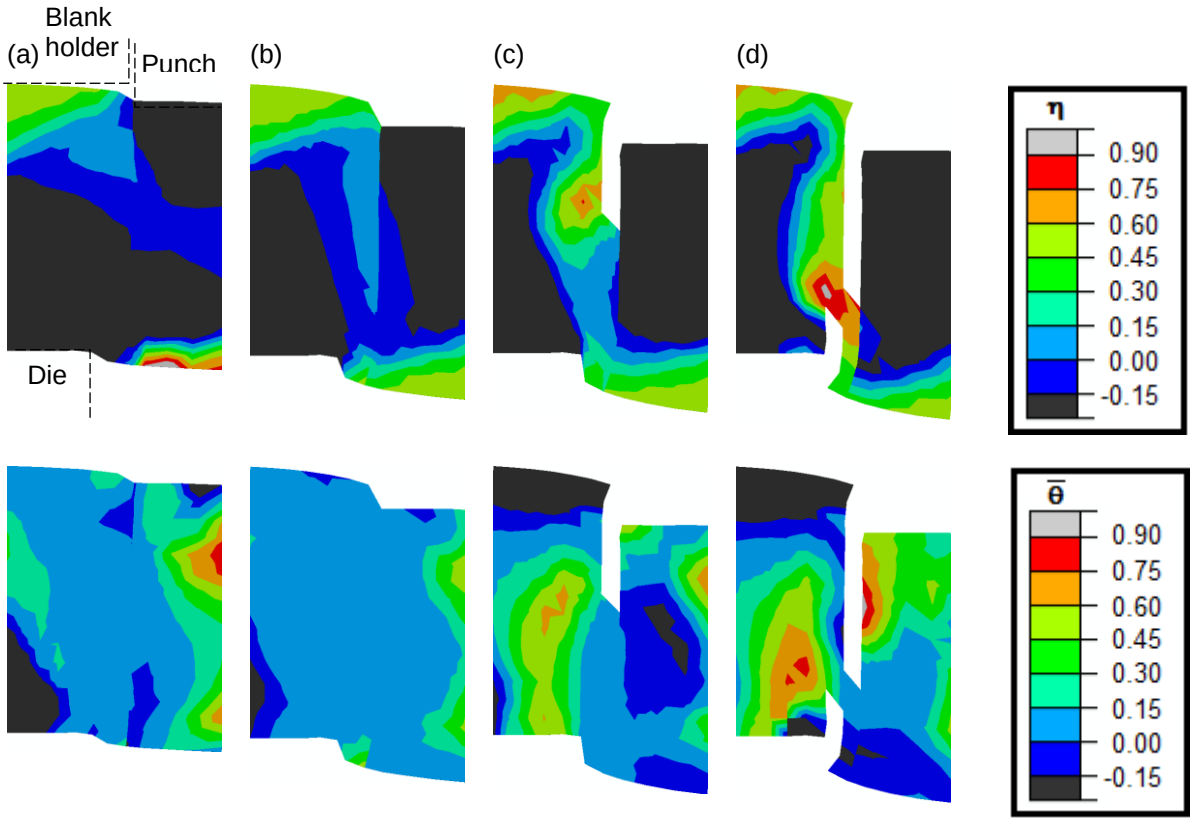

Figure 5. The stress state, in terms of stress-triaxiality and normalized Lode angle parameter, in different steps of blanking process (the figures were captured from the view, which was shown in figure 4 by a black dashed rectangular). The frames before the damage initiation, the crack initiation, the second crack initiation, and the material's final separation are shown in (a) to (d), respectively.

The crack initiated from the element in adjacent to the punch and grew towards the direction of cutting, figure 5(c). Meanwhile, a second crack initiated from the other side of the thickness and grew upwards, figure 5(d). The formation of the second crack prevented the burr surface from expanding. The stress-state from crack initiation until the entire separation changed from pure-shear mode to plane-strain state [14]. The new surface which was created under pure shearing is called clean-shear. The rest of new surface is called fracture surface.

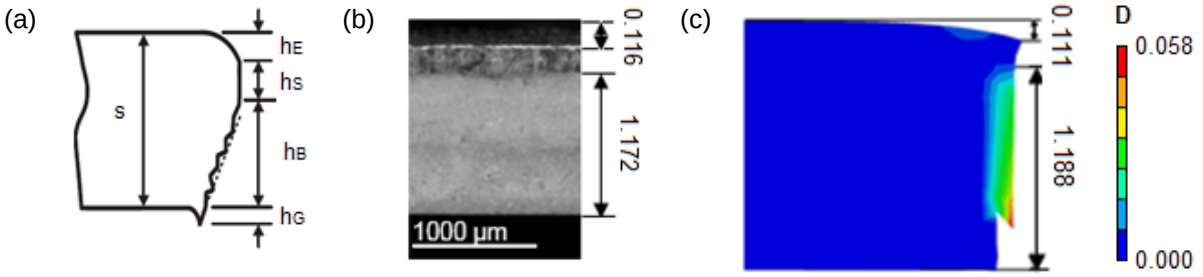

Figure 6. The blanked surface characteristics (a) h_E, h_S, h_B, h_G represent height of rollover, clean-shear, fracture, and burr parts, respectively [14]. S is the initial thickness of sheet; (b) the experimental data which was measured with accuracy of 1.0 µm [10]; and (c) the simulation results in terms of damage parameter (all dimensions are in mm).

2.5. EFTT process: Tension stage

The manufactured EFTT specimen undergoes uniaxial tensile test in the second stage. The specimen is expected to fail earlier than a uniaxial tensile specimen which is manufactured by milling process in both sides [12]. Results of the simulation are compared with experimental data in figures 7 and 8, which imply that the simulation approach was quite reliable.

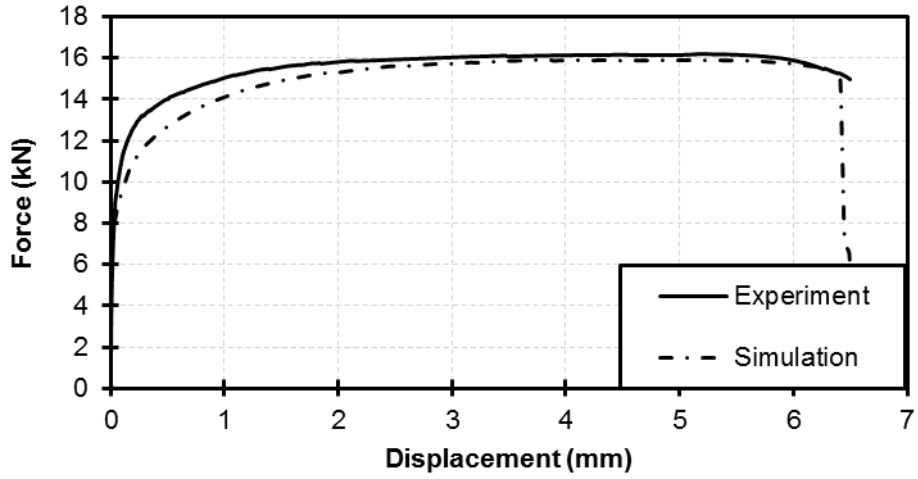

Figure 7. The comparison between *Edge-Fracture-Tensile-Test* results for experiment and simulation.

The effect of predamage is obvious in figure 8, which shows that damage initiated from the blanked edge. First, the crack propagated a little bit diagonally, then soon it grew perpendicularly to the loading direction and crossed the specimen. The same trend can be seen in the experiments as well. The experimental values of ε_1 which were taken by DIC are slightly higher than the simulation's values, as the DIC method is less sensitive and accurate in comparison to the simulations. In brief, the location and moment of fracture are predicted precisely by this method. Figure 9 illustrates that the damage and fracture initiated from the part of thickness which underwent the highest residual damage from the cutting process, i.e. the transition part of fracture to burr. Multiple cracks initiated along the shear cut edge during the *Edge-Fracture-Tensile-Test*.

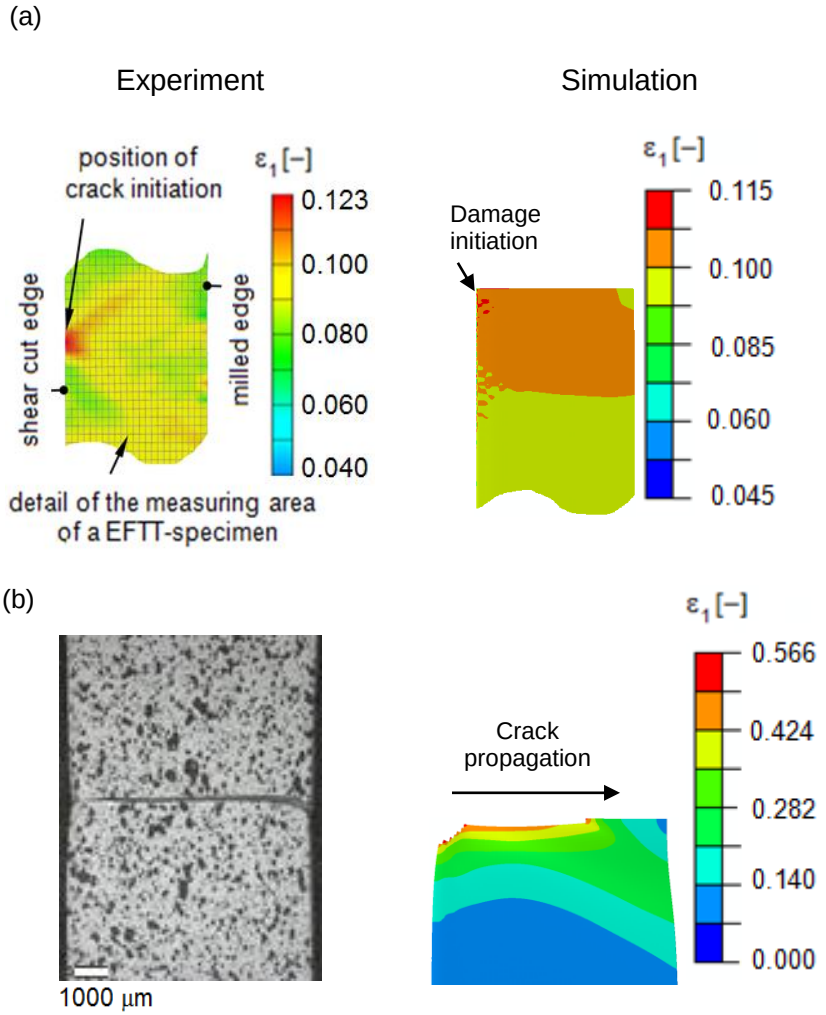

Figure 8. The comparison between experimental and simulation results of (a) damage initiation, and (b) fracture.

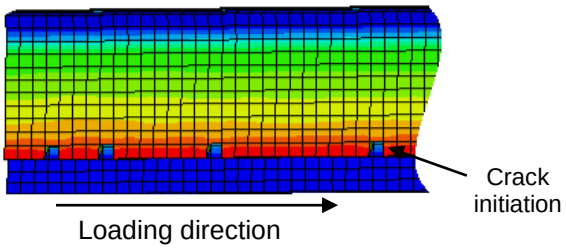

Figure 9. The view of EFTT specimen along the cut edge implies that the cracks initiated at the transition part from the fracture to the burr during the subsequent tensile test.

3. Conclusion

The presented study introduces a promising numerical tool for assessing the influences of the blanking process on formability of a component through *Edge-Fracture-Tensile-Test*. The important findings of this work are summarized below.

- The simulation of the blanking process by using MBW plasticity model provided detailed information of material's stress-state during the whole process. It showed that the damage and fracture initiated in the near shear state and changed gradually to the plane-strain mode until ultimate separation happened.

- The geometry features of the blanked edge, including rollover, clean-shear, fracture, and burr, were properly calculated by the simulation.
- The simulation of the subsequent uniaxial tensile test was able to predict the force-displacement curve and the damage behavior of the EFTT specimen in terms of location and moment of the damage.
- This numerical method along with MBW model could acquaint researchers with sound data of edge crack sensitivity which is one of the serious challenges of producing complicated components from HSSs.

Acknowledgement
The authors would like to thank Dr. Bo Wu from IWM institute of RWTH-Aachen University for his kind contribution.

Reference

[1] Nasheralahkami S, Golovashchenko S, Pan K, Brown L and Gugnani B 2016 *SAE Int.* 2016-01-0358
[2] Hasegawa K, Kawamura K, Urabe T and Hosoya Y 2004 ISIJ Int. **44** 603
[3] Casellas D, Lara A, Frómeta D, Gutiérrez D, Molas S, Pérez L, Rehrl J and Suppan C 2017 *Metall. Mater. Trans.* A **48** 86
[4] Karelova A, Krempaszky C, Werner E, Tsipouridis P, Hebseberger T and Pichler A 2009 *Steel Res. Int.* **80** 71
[5] Wang K, Luo M and Wierzbicki T 2014 *Int. J. Fracture* **187** 245
[6] Wang K, Greve L and Wierzbicki T 2015 *Int. J. Solids. Struct.* **71** 206
[7] Sartkulvanich P, Kroenauer B, Golle R, Konieczny A, Altan T 2010 *CIRP Annals – Manufact. Tech.* **59** 279
[8] Hu X, Sun X and Golovashchenko S 2016 *FE Anal.Des.* **109** 1
[9] Hu X, Sun X and Golovashchenko S 2014 *Comput. Mater. Sci.* **85** 409
[10] Feistle M, Golle R and Volk W 2016 *Procedia CIRP* **41** 1078
[11] Feistle M, Krinninger M, Paetzold I, Stahl J, Golle R and Volk W 2017 *J. Phys.: Conf. Ser. (Munich)* vol 896 (IOP Science) p 012106
[12] Feistle M, Krinninger M, Pätzold I and Volk W 2015 Edge-fracture-tensile-test *60 Excellenct Invention in Metal Forming* ed Tekkaya A et al (Berlin, Heidelberg: Springer Berlin Heidelberg) pp 193-198
[13] Wu B, Li X, Di Y, Brinnel V, Lian J and Münstermann S 2017 *Fatigue Fract. Eng. Mate. Struct.* **40** 2152
[14] N N 1994 Quality of cut faces of (sheet) metal parts after cutting, blanking, trimming or piercing, shearing form of sheared edge and characteristic *values Association of Engineers* (Berlin: Beuth Verlag GmbH) VDI 2906-2
[15] Gutknecht F, Steinbach F, Hammer T, Clausmeyer T, Volk W and Tekkaya A E 2016 *Procedia S truct. Integ.* **2** 1700